Self-induced gaps and optical bistability in semiconductor superlattices

Pawel Hawrylak
Division of Physics, National Research Council of Canada, Ottawa, Ontario, Canada K1A 0R6

Marek Grabowski
Department of Physics, University of Colorado, P.O. Box 7150, Colorado Springs, Colorado 80933-7150

(Received 14 June 1989)

We consider a semiconductor superlattice built of quasi-two-dimensional layers of narrow-band-gap material sandwiched by barriers of wide-band-gap material. We show that when the electromagnetic wave with frequency below the band gap of the superlattice propagates along the superlattice axis, it induces intensity-dependent gaps in the spectrum. The connection between these unusual gaps and spatial chaos is explored. The possibility of bistable devices is discussed.

The concept of optical bistability[1] is important both for optical switching, logic, and signal processing and the exploration of various routes to chaos. Optical bistability results from the nonlinear response of the medium to incident radiation. The nonlinearity may arise either via resonant (absorptive) or nonresonant (dispersive or Kerr) excitation. Recently both the room-temperature excitonic optical bistability in GaAs-$Ga_{1-x}Al_xAs$ multiple quantum wells[2] and nonresonant optical nonlinearities[3] have been observed and studied theoretically. These studies were focused predominantly on the microscopic origins of the phenomenon and reduced dimensionality of a single quantum well. The superlattice aspect of this problem is addressed here. The related problem of the optical response of dielectric superlattices[4] constructed from layers with different, intensity-dependent, dielectric constants has been studied theoretically. The authors of Ref. 4 were, however, primarily concerned with the effects of dispersive nonlinearities on stop gaps of a linear theory.

We present here a new approach emphasizing the three crucial aspects of optical bistability in nonresonantly excited multiple quantum wells: the spatial periodicity, discreteness, and nonlinearity. We do so by considering a phenomenological model which is trivial in the absence of either periodicity[5] or nonlinearity but yields unusual results when both effects are present. Such a situation can be realized in semiconductor quantum wells by the excitation of virtual exciton states concentrated mainly in the narrow layers of a lower gap material.[3]

The superlattice is modeled by an array of N very thin, nonlinear layers, positioned at $z=la$, where $l=1, 2, \ldots, N$ and a is the layer separation. The space between layers is filled with a medium of dielectric constant ϵ^0 independent of the intensity of the electric field. The system is placed in a Fabry-Perot cavity with mirrors of reflectivity r and transmittivity t $(1=t^2+r^2)$ located at $z=0$ and $z=a(N+1)$. The dielectric constant ϵ^1 of nonlinear layers depends on the intensity of the electromagnetic wave as $\epsilon^1=\epsilon^0(1+gEE^*)$, where g is the nonlinear coefficient (coupling constant).[3,4] The stationary wave equation describing the propagation of a transverse electromagnetic wave E in the superlattice can now be written as

$$\frac{d^2E}{dz^2}+k^2E=-gk^2EE^*E\sum_{l=1}^{N}\delta(z-la)\ , \tag{1}$$

where $k=(\epsilon^0\omega^2/c^2)^{1/2}$ is the wave vector of a wave with frequency ω in the linear medium, and c is the speed of light. We wish to emphasize that both the nonlinearity and periodicity are introduced on the same level and neither one can be treated as a perturbation. The equation of motion for the complex electric field has a useful mechanical analog. It can be viewed as describing a degenerate pair of harmonic oscillators, kicked periodically with a force depending on the displacement.

Because the medium between the layers has linear response, we can write the solution to Eq. (1) between layer m and $m+1$ in the form $E_m(z)=A_m\exp[ik(z-ma)]+B_m\exp[-ik(z-ma)]$. The relation between (A_{m-1},B_{m-1}) and (A_m,B_m) can be obtained by integrating Eq. (1) across the mth layer and using the continuity of E. After some algebra we have

$$A_{m-1}=e^{-ika}[A_m-\tfrac{1}{2}kgi|A_m+B_m|^2(A_m+B_m)]\ , \tag{2}$$

$$B_{m-1}=e^{+ika}[B_m+\tfrac{1}{2}kgi|A_m+B_m|^2(A_m+B_m)]\ . \tag{3}$$

For the transmission problem, the boundary conditions require an outgoing wave $E(z)=E_te^{ikz}$ outside the cavity [for $z>(N+1)a$], where E_t is the amplitude of the transmitted wave. Matching the fields across the ideal mirror yields the initial conditions for the map given by Eq. (2): $A_N=E_te^{ikNa}/t$, $B_N=E_te^{-ikNa}r/t$. The initial condition is then propagated backwards N times to obtain A_0 and B_0. The electric field for $z<0$ is a superposition of the incident and reflected waves: $E(z)=E_ie^{ikz}+E_re^{-ikz}$. The amplitude of the incident wave can now be expressed in terms of A_0 and B_0 as $E_i=A_0/t-B_0r/t$ hence it can be related to the amplitude of the transmitted wave or vice versa. This simple procedure allows us to easily *calculate* the transmitted intensity as a function of the incident intensity and thus to obtain the nonlinear transmission coefficient

$T=|E_t|^2/|E_i|^2$. These functions turn out to be very complex as we shall demonstrate below and the *understanding* of their complexity can be accomplished by drawing analogies to the dynamics of the chaotic, conservative systems.[6–9]

The discrete map given by Eqs. (1)–(3) results from the coupling between the gradient and the electric field across the mth layer. The dimensionality of this map can be reduced due to the global gauge invariance of Eqs. (2)–(3). This is accomplished by the choice of new variables: $Q=X+Y$, $R=X-Y$, Z, and J. The variable X is the intensity of the electromagnetic wave, $X=|A+B|^2$, the variable Y is proportional to the amplitude of the gradient, $Y=|A-B|^2$, and the conjugated variables Z and J are defined as $Z=2\,\mathrm{Im}[(A^*+B^*)(A-B)]$ and $J=2\,\mathrm{Re}[(A^*+B^*)(A-B)]$. The quantity J is simply related to the rate of energy flow S along the superlattice axis as $S=Jc/16\pi$. Because there are no losses, J is invariant under the operation of the map (conservative system) and we obtain a three-dimensional (3D) map:

$$Q'=Q-gkXZ+(gk)^2X^3\,, \tag{4}$$

$$R'=+\cos(2ka)R+[\sin(2ka)+Xgk\cos(2ka)]Z -S(X)kgX^2\,, \tag{5}$$

$$Z'=-\sin(2ka)R+[\cos(2ka)-Xgk\sin(2ka)]Z -C(X)kgX^2\,, \tag{6}$$

$$S(X)=2\sin(2ka)+kgX\cos(2ka)\,, \tag{7}$$

$$C(X)=2\cos(2ka)-kgX\sin(2ka) \tag{8}$$

with $X=(Q+R)/2$. Equations (4)–(6) describe a three-dimensional, volume-preserving map. One of the consequences of the conservation of the current J is the presence of invariant surfaces σ: $0=J^2+Z^2+R^2-Q^2$. This constraint allows us to eliminate the variable Q from the 3D map and obtain a 2D map, trajectories of which correspond to a constant energy flow through the superlattice. An arbitrary choice of initial conditions for the 3D map simply selects the invariant energy surface and hence the value of J.

Let us now consider the transmission problem without mirrors ($r=0$). In the absence of nonlinearity ($g=0$) the plane-wave solution $E(z)=E_te^{ikz}$ corresponds to the point ($R=0$, $Z=0$, $Q=2|E_t|^2$) and $J=Q$. It is convenient to measure all variables in the units of the intensity of the transmitted wave. This replaces the nonlinear coupling constant g by $g|E_t|^2$ in Eqs. (4)–(6) and the initial condition for the plane wave becomes simply (0,0,2). We now ask if in the presence of nonlinearity the plane-wave solution remains bounded, i.e., whether it can describe a transmitting state. The initial condition for a given value of the wave vector ka and the coupling constant $g|E_t|^2$ is then iterated and the values of the wave vector and transmitted intensity for which the trajectory remains within a radius of 10 from the initial condition after 100 iterations are recorded. The result is shown in Fig. 1. For small values of ka practically all states are transmitting, but as the value of ka increases, gaps (white areas) begin to open. If we keep the wave vector constant there are several possible values of transmitted intensity. This is a manifestation of multistability. The overall structure of the gaps depends very weakly on the size of

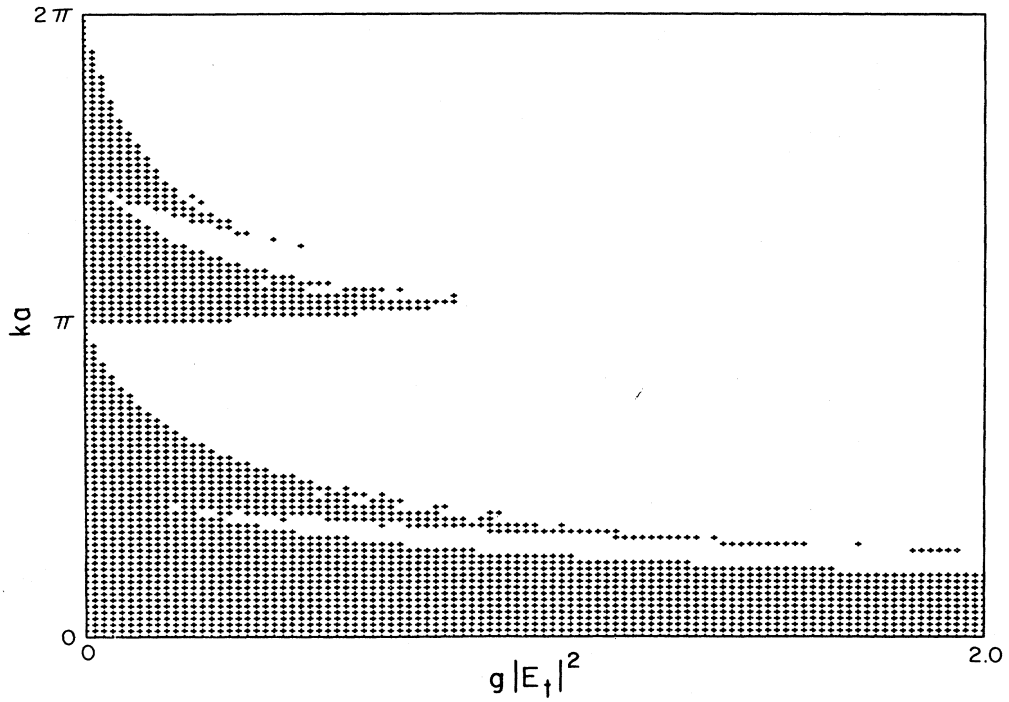

FIG. 1. Shown are the values of the wave vector ka and transmitted intensity $g|E_t|^2$ for which a nonlinear orbit generated by a three-dimensional map [Eq. (4) with $g=+1$] remained within a radius $r=10$ of a plane-wave initial condition after 100 iterations. Note the appearance of white regions which correspond to plane solutions being unstable and the system becoming opaque.

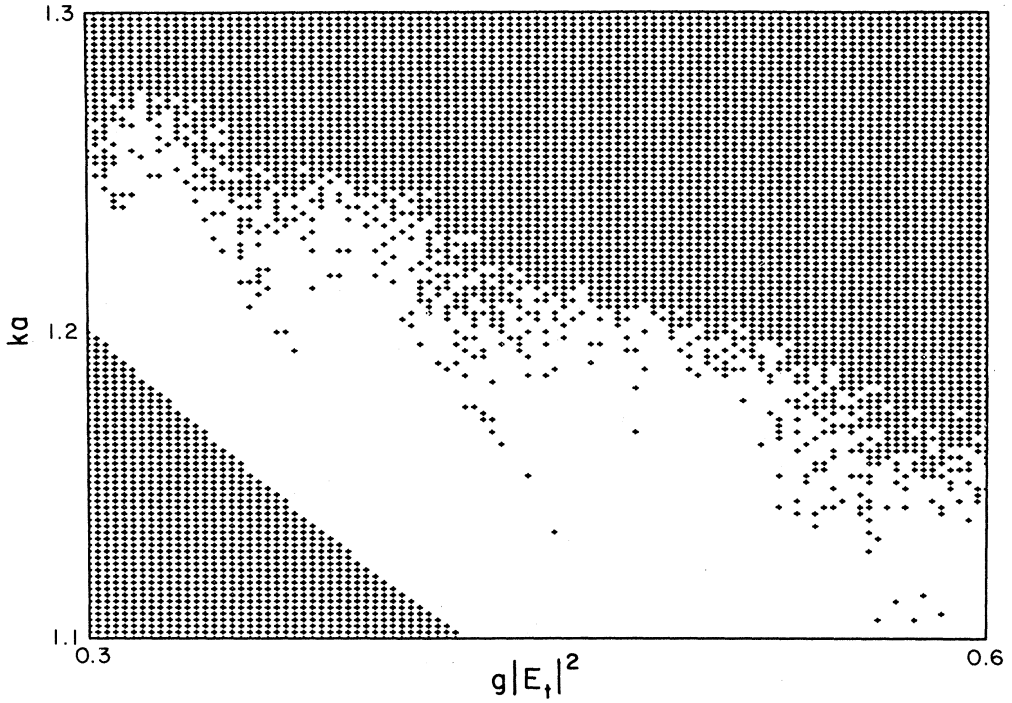

FIG. 2. The expanded view of the structure of one of the lowest gaps in Fig. 1 around $ka=1.2$.

the system N and the radius chosen. However, an increasingly complex structure emerges when small fragments of the gap region are magnified, as shown in Fig. 2, where we have selected the values of ka from 1.1 to 1.3 and the values of $g|E_t|^2$ from 0.3 to 0.6. These values correspond to the lowest visible gap in Fig. 1.

We now calculate the dependence of transmitted intensity on the incident intensity using Eqs. (2)–(3) for the value of the wave vector $ka=1.2$ ($r=0$, $g=+1$, $N=100$) corresponding to the gap in Fig. 2. As anticipated from Fig. 1 for low transmitted and incident intensities (less than 0.3) the system is transmitting. As the intensity exceeds 0.3 the sample becomes opaque to return to the transmitting state for the incident intensity range of 0.5–0.9. The transition from the transmitting state to a reflecting state is extremely sharp. However, in contrast to the continuous systems[5] one can find several very narrow transmitting states in the gap region, as is clear from the gap structure in Fig. 2. General features of the gap in the transmission spectrum are independent of the system size, the sign of the coupling constant (for $g=-1$ we find the gap at lower intensities), and the presence of mirrors.

The understanding of the origin of the nonlinear-induced gaps in the transmission spectrum can be obtained from analysis of the structure of the 3D discrete, nonlinear map. This is comprised of the understanding of the position and stability of fixed points and periodic orbits, basins of stability which contain quasiperiodic orbits, and the presence of stochastic layers known to exist in conservative systems.[6] In what follows we embark on a less ambitious task, i.e., we concentrate on the region in the vicinity of the plane-wave solution (0,0,2) for the range of parameters corresponding to the gap shown in Fig. 3.

In the absence of nonlinearity ($g=0$) the linear map corresponds to a rotation by $\phi=2ka$ in the (R,Z) plane leaving Q unchanged. Invariant surfaces are cylinders centered around the $(0,0,Q)$ line. This line is a collection

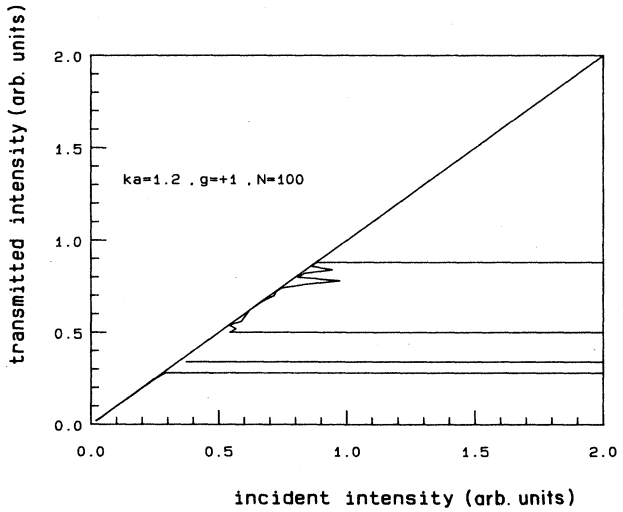

FIG. 3. The illustration of the multistability of the transmission. Shown is the transmitted intensity as a function of incident intensity for 100 layers and wave vector $ka=1.2$ (as in Fig. 2). The mirrors are fully transmitting ($t=1$). Note the opening of a gap in the spectrum for incident intensities between 0.3 and 0.5.

of elliptic fixed points. The nonlinearity breaks the symmetry of the linear transformation and moves the elliptic fixed point. For small values of the coupling constant $g|E_t|^2$ the initial point remains in the basin of stability of the fixed point. The value $g|E_t|^2=0.3$ corresponds to the case when the initial point has left the basin of stability of the fixed point of the map. In Fig. 4(a) we show examples of the trajectories generated by a 3D map projected on the (R,Z) plane. The deformed ellipses mark the basin of stability of the fixed point. The initial point is on the edge of the basin. We should remember that these orbits correspond to different values of current J. As the coupling constant increases the initial point remains outside the basin of stability of the fixed point resulting in escaping orbit (a gap in the transmission spectrum). As the coupling constant increases further the fixed point undergoes a bifurcation and period doubling.

For the coupling constant $g|E_t|^2>0.5$ the initial point enters the basin of stability of the periodic orbit and becomes a transmitting state again.

We illustrate the trajectories in the (R,Z) plane in the presence of a doubly periodic point in Fig. 4(b). The initial point is in the basin of stability of the lower periodic point. We also note the presence of a stochastic layer surrounding these two periodic points. This layer is partially responsible for the fuzziness of the upper edge of the gap in Fig. 2. We stress that the transition from low to high transmitting state as shown in Fig. 3 is associated with period doubling. The effect of mirrors is to move the initial point from the origin so the position of the gap versus ka or coupling constant may change but the basic mechanism remains the same.

In summary, we have shown that the electromagnetic wave with the frequency below the band gap of the superlattice can induce gaps in the transmission spectrum. These nonperturbative gaps arise from the combined effects of periodicity and nonlinearity and lead to optical multistability. The gaps can be tuned by changing the separation between layers, the strength of nonlinearity, and the properties of the cavity. Their origin has been linked to a complex dynamics of a discrete, nonlinear map. While much remains to be learned about the connection of this problem to the spatial chaos, it is hoped that this tunable mechanism will lead to a new class of optically bistable devices and better understanding of chaos in condensed mater.

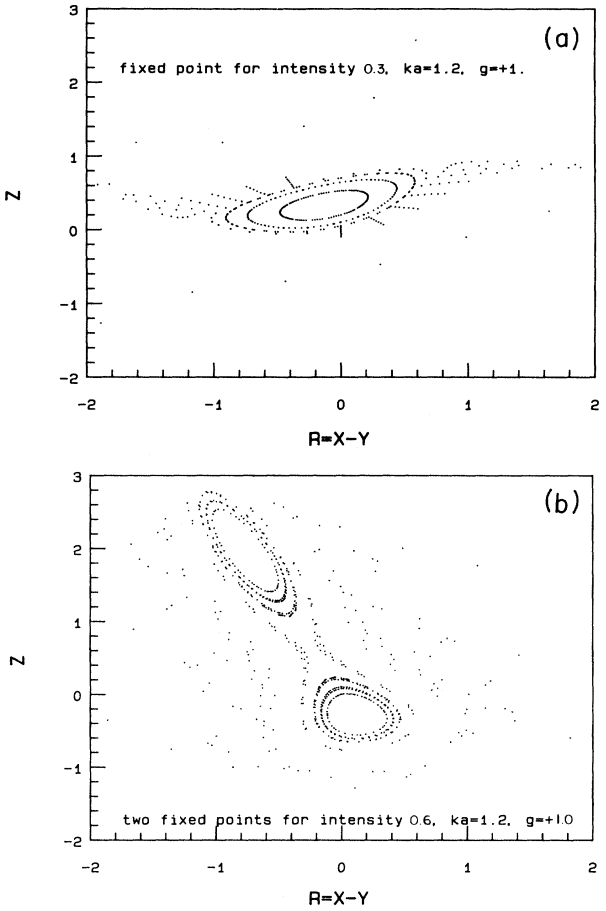

FIG. 4. The projection of trajectories on the (R,Z) plane of a 3D map for various initial conditions. (a) $g|E_t|^2=0.3$, i.e., the onset of the gap in Fig. 3. Note that the initial condition (0,0,2) of a plane wave is just leaving the basin of stability of an elliptic fixed point. Hence the escaping orbit and the sharp onset of the gap in the transmission spectrum. (b) For $g|E_t|^2=0.6$, i.e., in the center of a top transmitting region in Fig. 3. Note the presence of two periodic fixed elliptic points which bifurcated from the fixed point seen in (a) as coupling constant $g|E_t|^2$ is increased. The initial condition is in the stability basin of the lower fixed point.

M. G. acknowledges partial support by U.S. Army Research Office (ARO) Grant No. DAAL03-88-K-0061 and also the hospitality and partial support of the Microstructural Sciences Laboratory, Division of Physics, National Research Council of Canada.

[1]For a review see C. Flytzanis, in *Nonlinear Phenomena in Solids—Modern Topics,* edited by M. Borissov (World Scientific, Singapore, 1986), p. 268.

[2]D. S. Chemla, D. A. B. Miller, P. W. Smith, A. Gossard, and W. Wiegmann, J. Quantum Electron. **20**, 265 (1984).

[3]C. Ell, J. F. Muller, K. El Sayed, and H. Haug, Phys. Rev. Lett. **62**, 304 (1989); S. Schmitt-Rink and D. S. Chemla, *ibid.* **57**, 2752 (1986); A. Mysyrowicz, D. Hulin, A. Antonetti, A. Migus, W. T. Masselink, and H. Morkoç, *ibid.* **56**, 2748 (1986); M. Combescot and R. Combescot, *ibid.* **61**, 117 (1988).

[4]Wei Chen and D. L. Mills, Phys. Rev. Lett. **58**, 160 (1987); Phys. Rev. B **36**, 6269 (1987); D. L. Mills and S. E. Trullinger, *ibid.* **36**, 947 (1987).

[5]F. S. Felber and J. H. Marburger, Appl. Phys. Lett. **28**, 731 (1976).

[6]Alexander A. Chernikov, Roald Z. Sagdeev, and George M. Zaslavsky, Physics Today **41**, 27 (1988).

[7]Robert L. Devaney, *An Introduction to Chaotic Dynamical Systems* (Benjamin/Cummings, Menlo Park, CA, 1986).

[8]Francois Delyon, Yves-Emanuel Levy, and Bernard Souillard, Phys. Rev. Lett. **57**, 2010 (1986).

[9]P. Hawrylak, M. Grabowski, and P. Wilson, Phys. Rev. B **40**, 6398 (1989).